Journal of Sustainability for Energy
https://www.acadlore.com/journals/JSE

Enhancement of Pool Boiling Heat Transfer via Water-Based Nanofluids and Multi-Finned Surface Geometries

Hamzah Hadi Fadhl[1], Laith Jaafer Habeeb[2*]

[1] Mechanical Engineering Department, Faculty of Engineering, Shahid Chamran University of Ahvaz, 6135783151 Ahvaz, Iran
[2] Training and Workshop Center, University of Technology-Iraq, 10066 Baghdad, Iraq

* Correspondence: Laith Jaafer Habeeb (Laith.J.Habeeb@uotechnology.edu.iq)

Received: 03-12-2024 **Revised:** 04-29-2024 **Accepted:** 05-10-2024

Citation: H. H. Fadhl and L. J. Habeeb, "Enhancement of pool boiling heat transfer via water-based nanofluids and multi-finned surface geometries," *J. Sustain. Energy*, vol. 3, no. 2, pp. 105–118, 2024. https://doi.org/10.56578/jse030204.

© 2024 by the author(s). Published by Acadlore Publishing Services Limited, Hong Kong. This article is available for free download and can be reused and cited, provided that the original published version is credited, under the CC BY 4.0 license.

Abstract: In the realm of heat transfer, the phenomenon of boiling heat transfer is paramount, especially given its efficiency in harnessing the latent heat of vaporization for significant thermal energy removal with minimal temperature alterations. This mechanism is integral to various industrial applications, including but not limited to the cooling systems of nuclear reactors, macro- and micro-electronic devices, evaporators in refrigeration systems, and boiler tubes within power plants, where the nucleate pool boiling regime and two-phase flow are prevalent. The imperative to optimize heat exchange systems by mitigating excessive heat dissipation, whilst simultaneously achieving downsizing, has consistently been a critical consideration. This research uses computational, based on Fluent software, to analyze thermal characteristics and cooling mechanisms of different concentrations of nanofluids, in conjunction with surfaces adorned with diverse fin geometries. Specifically, the study scrutinizes the thermal performance of water-based nanofluids, incorporating Copper (II) Oxide (CuO) nanoparticles at concentrations ranging from 0% to 1.4% by volume, under boiling conditions. The analyses extend to the efficacy of different fin shapes—including circular, triangular, and square configurations-within a two-dimensional geometry, under the conditions of forced convection heat transfer in both steady and transient, viscous, incompressible flows. The findings are poised to contribute to the design of more efficient heat exchange systems, facilitating enhanced heat dissipation through the strategic use of nanofluids and meticulously designed surface geometries.

Keywords: CuO; Nanoparticles; Heat transfer coefficient (HTC); Pool boiling; Multi-fin geometries; Nanofluids

1 Introduction

Pool boiling is a tempting cooling method for high-heat flux components, such as computers and other electrical gadgets. Due to the phase change phenomenon's better heat rate, boiling has been extensively used as the primary heat transfer mechanism in two-phase thermal systems. In order to save energy and keep such systems lasting, heat transfer performance must be intensified during boiling. Numerous studies have previously attempted to solve this issue, but the high expense of nanofluids made the trials unfeasible. The fluid dynamics of heat transfer and cooling processes were also anticipated in this study through numerical analysis. This offers the possibility of using more nanofluid concentrations and various geometric shapes of the fins, and to experiment at a lower cost with multiple base fluids and nanofluids.

Eid et al. [1] used the nucleate pool boiling HTC to look into how adding CuO changed the HTC of the refrigerant R-134a. A mirror surface roughness (Ra) of 0.042 µm was used in the studies using a flat heating surface. 0.005, 0.01, 0.03, and 0.05 percent by volume of CuO particles were used. Different operational boiling pressures and heat fluxes (ranging from 15 to 150 kW/m^2) are used. As the concentration of CuO particles increased from 0.005% to 0.03%, the findings showed that the HTC rose. The improvements reach 82% when the nanoparticle concentration is increased to 0.03% by volume at a high heat flux of 150 kW/m^2. As a result of the substantial amount of nanoparticles deposited on the heating surface, the HTC dropped when the volume concentration of CuO nanoparticles was raised to 0.05 percent.

Kamel and Lezsovits [2] studied experimental performance (PBHTC) employing a cerium oxide-based water nanofluid from a horizontal copper-heated tube in 2020. The boiling curves and (PBHTC) for DI water and nanofluid at various concentrations. The amounts of nanoparticles utilized in this investigation were between 0.001 and 0.04 percent vol. The results showed that the PBHTC of nanofluids and pure water went up as the heat flux went up. This is because bubbles formed during the nucleate boiling regime. Additionally, the PBHTC of nanofluid was increased at all volume concentrations, with a greater improvement found with a volume fraction (0.007 percent vol.) of nanofluid of around 1.7 utilizing the PBHTC enhancement ratio (PBHTCnf/PBHTC water) compared to DI water at low heat flux.

The heat transfer properties of the boiling pool of aqueous nanofluids with multiwalled carbon nanotubes on modified surfaces were studied by Sarafraz and Hormozi [3] and experimentally verified up to the critical point of heat flow. The diamond shape with micro-financed with different geometric shapes has been used to modify the surfaces. This reduced the HTC upon boiling at the normal surface but was improved up to 56 percent and 77 percent at wt. = 0.1 and wt. = 0.3, respectively, at the surfaces with micro-fins. Additionally, it was shown that the changed surfaces lowered pollutant rates when compared to the natural surface. Additionally, it was shown that these surfaces might also create a filthy, uneven layer, which increased the number of active nucleation sites for bubble production. Nevertheless, on a typical surface, a continuous fouling layer forms, significantly reducing the HTC due to the high thermal resistance it introduces. The surface properties changed when carbon nanotubes were added. For example, it became more wettable and the static contact angle value went down. In this scenario, the critical heat flow (CHF) may be enhanced by as much as 95% (wt percent = 0.3). In addition to lowering the static contact angle and boosting the bulk concentration of nanofluids, While it is possible to speed up the bubble-making process, tests have shown that the formed bubbles may still exit the surface, leading to an increase in the HTC because of the localized agitation and the available heat transfer area.

Xie et al. [4], by cultivating nanograss as the substructure and microflowers with varying cover densities as the superstructure, the study decouples the contributions of intrinsic surface wettability and the hierarchical (dual-layer) structure to the boiling increase. The structured surfaces exhibit a 68 percent increase in CHF. While for multi-oriented (from 0° to 180°) substrates, the downward-facing surface's boiling performance is inhibited. Additionally, downward-facing orientations of the nanograss surface exhibit increased CHT and HTC. Additionally, novel correlations for the prediction of downward-facing CHF based on the horizontal CHF are provided for future multi-oriented surface designs in advanced heat transfer applications.

Chun et al. [5] studied the effect of quenching type on heat fluxes at the quenching process of a platinum (Pt.) wire with a diameter of 0.25 mm and a length of 100 mm by heating the Pt. wire to 1000 ℃. The cooling and boiling curves were then obtained, and the water-based carbide (Sic) and silicon (Si) Nanofluids were suddenly cooled in water at concentrations of 0.01 and 0.001 vol.%. The results showed that the critical heat flux when using Si nanofluids was slightly higher when compared to water, whereas the critical heat flux in Si nanofluids was lower than water. It also showed that the heat fluxes of (pt.) wire coated with (Si) and (Sic) nanoparticles when quenched in water were higher than the heat fluxes of non-coated (pt.) wire when extinguished in water or (Si) or (Sic) nanofluids.

Touhami et al. [6] developed correlations in 2014 that take into account the influence of diameter. These correlations are compared to existing data on pool boiling outside of a horizontal tube. It was also shown that these surfaces might enhance the number of active nucleation sites and bubble production by forming an uneven and filthy layer. On the other hand, a typical surface had a persistent fouling layer that significantly lowered the HTC by increasing thermal resistance. The surface properties were also changed by the addition of carbon nanotubes. For example, the surface became more wet and the static contact angle value went down. With a weight percentage of only 0.3, the CHF may be enhanced to a level of 95%. In addition to lowering the static contact angle and building up the mass concentration of nanofluids, A faster rate of bubble development is possible, according to tests; nevertheless, the formed bubbles may exit the surface, leading to a higher HTC because of the local agitation and the available heat transfer area. Saturated-liquid horizontal cylindrical heaters may be simplified by using these correlations, which are applied for each material. A specific equation may be derived based on the design parameters, and roughness is assumed to be 1 mm when not stated.

Zandabad et al. [7] studied the effect of the input pressure, mass flux, and inlet sub-cooling on the diameter of the bubble departure, the quadruple magnetic field, and the frequencies. The diameter change and frequency of bubble departure were found to be the same in the presence and absence of the magnetic field, indicating that the bubbles exhibited controlled growth in the field. In the presence of a sub-cooled magnetic field, the frequency of bubble departure rose by 45.45%, 30.38%, and 21.79% correspondingly, while the diameters of bubble departure reduced by 9.55%, 15.18%, and 15% compared to similar working circumstances without a magnetic field. In previous studies, the problem was tackled by many researchers whereby the use of nanofluids was economically expensive hence making the experiments costly. In the present work, computational fluid dynamics (fluent) was employed to analyze the heat transfer and cooling characteristics of the system, which provides a better chance to explore the application of higher concentrations of nanofluid and the utilization of various geometries of the fin.

Saieed et al. [8] focused on passive techniques to improve heat transfer in pool boiling using surface cavities and mechanical machining. A rectangular model and two models were created using Ansys Fluent. The volume of fluid multiphase model was used with Ethylene Glycol/water, Propylene Glycol/water, and water. Propylene Glycol/water had the highest pressure value in both vertical and horizontal boiling. Fadhl et al. [9] investigated the impact of working fluid, surface modification, and heat transmission in pool boiling microsystems, enabling electronic gadgets to increase processing capability while shrinking size. It uses nanofluids (Ethylene glycol + Al_2O_3 and Ethylene glycol + CuO nanofluids) and numerical investigation to analyze thermal performance during boiling conditions with different fin shapes. Results show best results for circular fins and 0.3% concentration of CuO + $C_2H_6O_2$ nanofluids. The boiling process, a crucial physical phenomenon, has gained importance in scientific physics due to its numerous uses. Majdi et al. [10] aimed to improve boiling in fluids using nanomaterials (CuO, Al_2O_3) in different concentrations. The study used three shapes of fins: rectangular, circle, and triangle. Results showed that increasing nanomaterial concentrations increased vapor velocity, pressure, and flow velocity. The best shapes provided more surface area for temperature. Boiling heat transfer is crucial for industrial applications like cooling devices, power plants, refrigerator, and nuclear power stations. Fadhl and Habeeb [11] used numerical simulations to study the heat transfer and cooling processes of nanofluids on finned surfaces. The study found that nanoparticles enhance thermal conductivity and surface area, leading to a higher heat transfer coefficient and reduced critical heat flux. However, the long-term stability and efficacy of nanofluids are affected by nanoparticle aggregation and sedimentation. These findings indicate the direction for future development of thermal management in different fields of industry.

This project's goal is to investigate how a working fluid affects a pool's surface modification and heat transfer at the same time. This is due to new developments in microsystems, which enable many electrical devices to raise their processing capacities as well as their size. However, these devices do raise the amount of heat loss per unit area to a very noticeable degree. In addition, enhance the HTC by employing nanofluid (CuO) with varied concentrations. Additionally, two types of base fluids are used, and surfaces with fins in the shapes of squares, triangles, and circles are used (water).

2 Numerical Analysis

The boiling HTC and CHF may be predicted using various relationships [12, 13]. Researchers studying boiling heat transfer with nanofluids [14–17] mostly compared their experimental findings to predictions from the Rohsenow [18] and Zuber [19] correlations. Thus, rather than discussing different hypotheses or correlations in depth, these two traditional correlations are offered here. Based on a three-dimensional study of all significant elements affecting nucleate boiling and experimental data obtained across a broad range of situations, Table 1 shows the properties of nanofluid CuO-water.

Table 1. Properties of nanofluid CuO-water

	Water	**Nanofluid CuO-Water**				
		Con. 0.3%	**Con. 0.6%**	**Con. 1%**	**Con. 1.2%**	**Con. 1.4%**
k	$0.613(\ \mathrm{W/mK})$	0.6080242	0.603075273	0.59651808	0.59325707	0.59000772
ρ	$999\ (\ \mathrm{kg/m^3})$	1013.509	1030.018	1052.030	1063.036	1074.042
c_p	$4217(\ \mathrm{J/kgK})$	4168.083	4157.166	4147.860	4128.0542	4135.332

2.1 Assumptions

(1) Temporary two-dimensional flow of a single phase working fluid in the pipe (homogeneous model).
(2) Newtonian fluid and incompressible.
(3) Constant temperature and neglect of viscous dissipation.
(4) The axial conduction along the enclosure is usually insignificant.
(5) There is no heat generation within the enclosure.
(6) The nanofluid is assumed to be incompressible with constant physical properties.
(7) The base fluid and nanoparticles are in thermal equilibrium, with the fluid phase and the nanoparticles moving at a constant relative velocity.
(8) Nanoparticles remain chemically stable at the molecular level with the base fluid.

2.2 CHF

The CHF situation occurs during wall boiling and is characterized by a considerable reduction in local HTC and an increase in the temperature of the wall surface. It happens when hot surfaces are no longer moistened by boiling liquid as the vapor concentration increases. When the heat flow is critical, vapor replaces the liquid and takes up residence next to heated walls. As a result, energy is transmitted through direct communication between the wall

and the vapor. As a consequence, the heat removal capacity rapidly decreases and the vapor temperature, and most crucially, the wall temperature, rapidly increases. Additionally, as the multi-phase flow regime changes from bubbly to misty, the wall boils away from the nucleating boiling regime.

ANSYS Fluent may be used to simulate critical heat flux and post-dry-out situations by extending There are a lot of steps in the RPI model that go from boiling to critical heat flux and then drying out:

• The partitioning of the wall heat flux into generalized and non-equilibrium conditions.

• The change of the flow regime from bubbly to mist flows.

2.3 Interfacial Momentum Transfer

Five components may contribute to interfacial momentum transfer: drag, lift, virtual mass, turbulent drift forces, and lubrication of the wall. There are several models for each of these phenomena, some of which are tailored particularly for boiling flows. Additionally, there are user-defined settings accessible [20].

2.3.1 Interfacial momentum transfer

A transport equation or an algebraic model may be used to compute the interfacial area. Algebraic models are often selected for boiling flow problems.

2.3.2 Bubble and droplet diameter

(1) Bubble diameter

For local subcooling, Fluent predicts bubble diameter using the following model:

$$D_b = \begin{cases} \max\left[1.0\times10^{-5}, d_{\min}\ \exp\left(\frac{-k(\Delta T_{\text{sub}}-\Delta T_{\max}}{d_{\min}}\right)\right] & \Delta T_{\text{sub}} > 13.5K \\ d_{\max} - K\left(\Delta T_{\text{sub}} - \Delta T_{\min}\right) & \Delta T_{\text{sub}} \le 13.5K \end{cases} \tag{1}$$

where:

$\Delta T_{\text{sub}} = T_{\text{sat}} - T_l$

$d_{\min} = 0.00015$ m

$d_{\max} = 0.001$ m

$\Delta T_{\min} = 0$ K

$\Delta T_{\min} = 0$ K

$\Delta T_{\max} = 13.5$ K

$K = \dfrac{d_{\max} - d_{\min}}{\Delta T_{\max} - \Delta T_{\min}}$

Alternatively, the bubble diameter may be used, D_b, may be determined by the Unal correlation:

$$D_b = \begin{cases} 0.0015 & \Delta T_{\text{sub}} < 0 \\ 0.0015 - 0.0001\Delta T_{\text{sub}} & 0 \le \Delta T_{\text{sub}} \le 13.5\text{ K} \\ 0.00015 & \Delta T_{\text{sub}} > 13.5\text{ K} \end{cases} \tag{2}$$

(2) Droplet diameter

There is a shift in the flow regime when mist is introduced, the diameter of the droplets may be considered constant or determined using the Kataoka-Ishii correlation:

$$D_d = C_{ds}\frac{\sigma}{\rho_v j_v^2}\,\text{Re}_l^{-1/6}\,\text{Re}_V^{2/3}\left(\frac{\rho_v}{\rho_l}\right)^{-1/3}\left(\frac{\mu_v}{\mu_l}\right)^{2/3} \tag{3}$$

where:

$C_{ds} = 0.28$

j_v vapor volumetric flux

Re_l Reynolds number for local liquid

Re_v Reynolds number for local vapor

μ_l viscosity of liquid

μ_v viscosity of vapor

(3) Interfacial drag force

The interfacial drag force is calculated using the standard model. ANSYS Fluent has a number of tools for computing the drag force on scattered phases. Typically, the Ishii model is utilized for boiling flows; however, any of the models are possible.

(4) Interfacial lift force

ANSYS Fluent has a number of methods for calculating the lift forces on scattered phases. This force is critical for boiling flows during the nucleating boiling regime. The Tomiyama model is often used in the RPI model for the lift force to be taken into consideration.

(5) Turbulent dispersion force

ANSYS Fluent includes a variety of different methods for calculating the turbulent dispersion force. This force is critical in transferring vapor from the walls to the core fluid flow areas in boiling flows. Typically, the Lopez de Bertodano model is used in the RPI model to account for the turbulent dispersion force.

(6) Wall lubrication force

For the purpose of calculating the wall lubrication force in scattered phases, ANSYS Fluent offers several methods. In the nucleating boiling regime for boiling flows, this force might be important. The RPI model frequently incorporates the Antal et al. model to take the effects of the wall lubricating force into consideration.

(7) Virtual mass force

The virtual mass force may be described in wall-boiling models utilizing the typical correlation developed for the Eulerian multi-phase model.

2.4 Interfacial Heat Transfer

2.4.1 Interfacial to liquid heat transfer

As the bubbles leave the wall and enter the subcooled zone, heat is transferred between the bubble and liquid.

$$\dot{q}_{\mathrm{lt}} = \mathrm{h_{sl}} \left(\mathrm{T_{sat}} - \mathrm{T_l} \right) \tag{4}$$

where, $\mathrm{h_{sl}}$ is the coefficient of volumetric heat transfer. The Ranz-Marshall or Tomiyama models may be used to calculate the HTC.

2.4.2 Interfacial to vapor heat transfer

The interface for vapor heat transfer is calculated using the constant-time scale return-to-saturation method. Many people think that the vapor quickly evaporates or condenses back to its saturation temperature. The formula is as follows:

$$\dot{q}_{\mathrm{vt}} = \frac{\alpha_{\mathrm{v}} \rho_{\mathrm{v}} \mathrm{C_{p,v}}}{\delta \mathrm{t}} \left(\mathrm{T_{sat}} - \mathrm{T_v} \right) \tag{5}$$

where, $\delta \mathrm{t}$ is the time scale set to a default value of 0.05 and $\mathrm{C_{p,v}}$ is the isobaric heat capacity.

2.5 Mass Transfer

2.5.1 Mass transfer from the wall to vapor

The evaporation heat flux is used to measure the evaporation mass flow, which is applied near the cell wall.

$$m_{\mathrm{E}} = \frac{\dot{q}_{\mathrm{E}}}{\mathrm{h_{fv}} + \mathrm{C_{p,1}} \Delta \mathrm{T_{sub}}} \tag{6}$$

2.5.2 Interfacial mass transfer

The passage of heat across interfaces is crucial for the movement of mass across them. The rate of mass transfer across interfaces may be expressed as follows: if all of the heat that is applied to the contact is used for mass transfer (evaporation or condensation):

$$m = \dot{m}_{lt} + \dot{m}_{vt} = \frac{\dot{q}_{\mathrm{lt}} + \dot{q}_{\mathrm{vt}}}{\mathrm{h_{fv}}} \tag{7}$$

3 Validation

By contrasting the findings with earlier findings from a different investigation that was repeated using the CFD program, the results were verified. The outcomes were nearly identical to those of the first investigation. $\mathrm{Al_2O_3}$-water nanofluids were used in the earlier investigation to improve calculate HTC boiling in the pool at low heat fluxes using response surface techniques. The two-phase Eulerian approach has been implemented, and bubble parameters are predicted using numerical simulation and experimental correlations, according to the publisher, Salehi and Hormozi [21]. The test pool's dimensions, the other solution parameter, and the boundary conditions are given in Figures 1- 3. A two-dimensional drawing of the computing domain was made, measuring 200 mm in diameter and 100 mm in height. The diameter of the boiling surface is 11 mm.

The $\mathrm{Al_2O_3}$-water nanofluid (0.3 mass $\%$) utilized had the following properties: nucleation site density $= 28\mathrm{l/m^2}$ and departure frequency $= 30\mathrm{l/s}$. The heat flux evaluated was between 30 and $200\,\mathrm{kW/m^2}$. The nucleation site density was the most remarkable bubble parameter, whereas the bubble departure diameter was the least

useful one. For discretization, control volume was utilized, convective expressions were handled by QUICK, and velocity-pressure coupling was handled by SIMPLE. Less than 10^{-6} coverage requirements apply to the continuity, momentum, and energy equations. Pool boiling HTC was used to test the mesh independence. At 100×160 cells, grid independence was attained with $\mathrm{q} = 50\ \mathrm{kW/m^2}$.

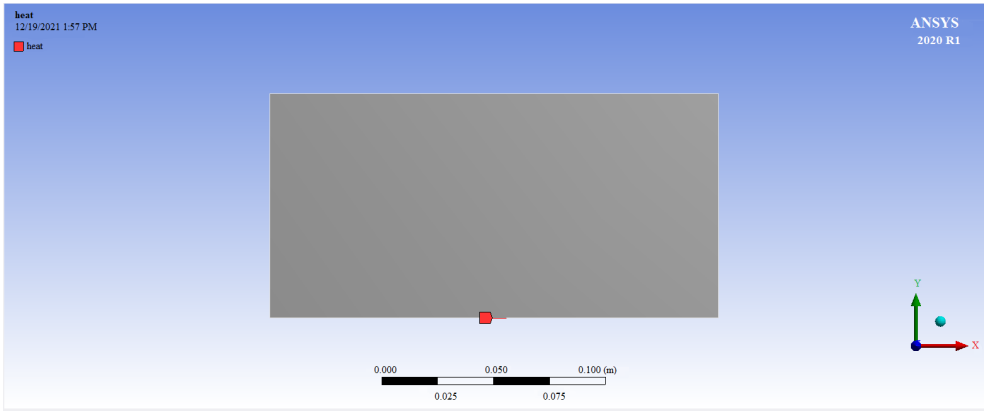

Figure 1. The location of heat flux

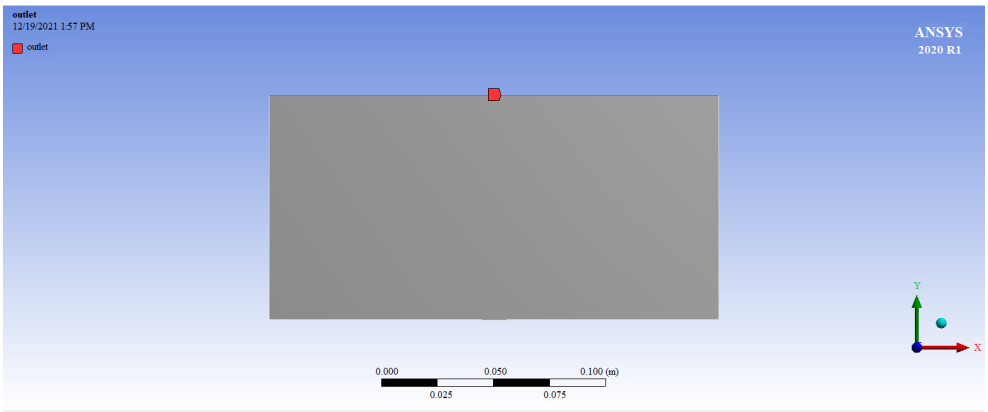

Figure 2. The type of boundary condition of lateral wall

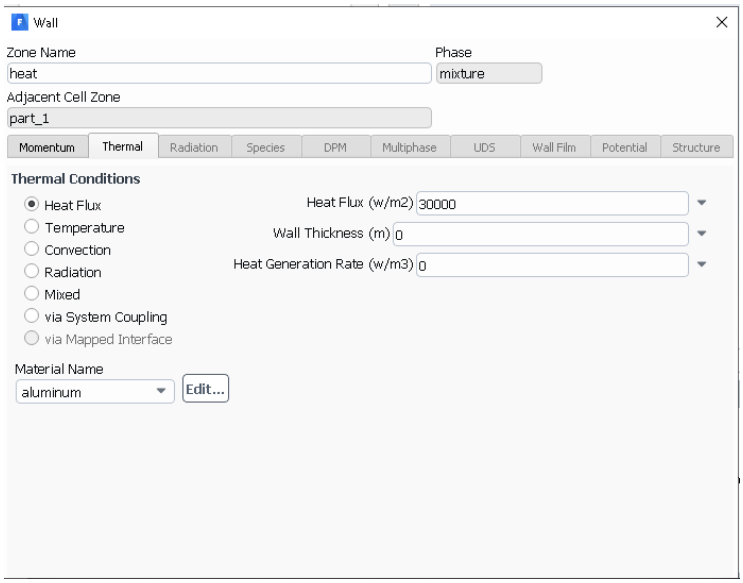

Figure 3. Heat flux added

The numerical results in this study were compared with Salehi and Hormozi's numerical results [17], which are shown in Table 2.

Table 2. Comparison of HTC that were obtained by this study with the previous results at the same values for applied heat flux

Heat Flux $(\mathbf{kW/m^2})$	**HTC** $(\mathbf{W/m^2 \cdot K})$ **from Current Numerical Results**	**HTC** $(\mathbf{W/m^2 \cdot K})$ **from Salehi and Hormozi Results**
30	340	363
80	680	720
130	1200	1358
180	1450	1580

4 Results and Discussion

In this work, nanofluids were introduced to base fluid, where two different types of nanofluids—distilled water and water—were used using numerical simulation to determine the phenomena associated with heat transfer. The simulations took five seconds to complete. In addition, copper oxide was employed as a nanomaterial in five different concentrations with varying percentages of water coolant (0, 0.3, 0.6, 1, 1.2, and 1.4%).

The following will be considered while reviewing the results:

(1) Nanofluid Concentration generally uses nanoparticles to create a layer on surfaces that decreases bubble formation and continually hydrates the surface, increasing the HTC and maintaining a steady temperature for the electronic devices that employ these nanomaterials for better cooling.

(2) Fins shape: There are three different kinds of geometric forms that were utilized in the mesh that were compared: square, circular, and rectangular shapes. The working fluid in this study is subjected to high temperatures within an integrated micro-finned enclosure, which makes up the system geometry. Examined the issue of nanofluids inside a finned enclosure of 20 mm in height and 37.5 mm in length. Fins come in three different varieties: square, round, and triangle, see figure 4. As seen in the figure, the diameter of the circular fin, the height and base of the triangular fin, and the width and height of the square fin all have identical measurements of 0.3 mm (4). These values, variables, and shapes were chosen based on previous research and the best surface area available.

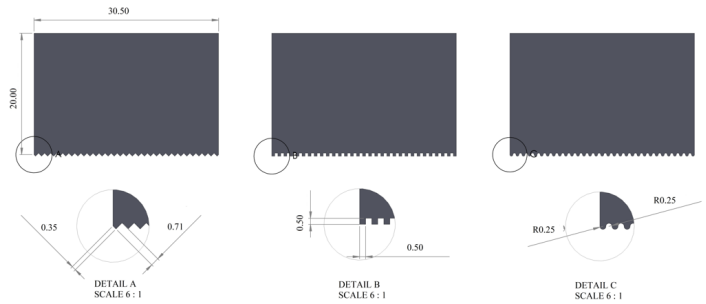

Figure 4. Physical geometry of finned enclosure

A 2-D geometry is produced, then structured and unstructured meshes are used to mesh the geometries. As illustrated in Figure 5, it is braided into a number of nodes and components.

The use of 2D geometry for fin analysis introduces simplifications that may not fully capture the complexities of the actual physical system, which is inherently three-dimensional. In a three-dimensional system, boundary layer effects may vary along different axes, leading to non-uniform heat transfer distributions. Three-dimensional effects can result in variations in temperature gradients across different planes of the fin. The 3D nature of the physical system affects the heat dissipation at the fin edges, where heat transfer occurs not only along the fin surface but also in the lateral direction. In a three-dimensional system, heat conduction through the substrate beneath the fin can play a significant role in overall heat transfer. The 3D nature of the physical system influences flow dynamics, particularly in the vicinity of the fin.

The elements for the three fin types are: square (74442), circular (159945), and triangular (74669). The computational model's geometry is created by creating a two-dimensional model of the fluid domain with SolidWorks software.

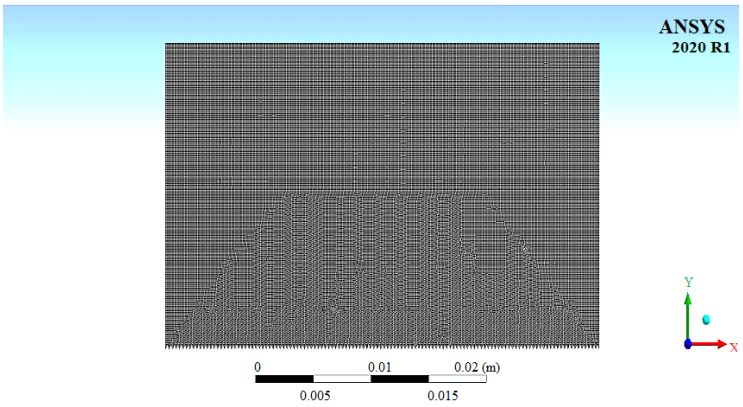

Figure 5. Meshing geometry created by Ansys-Workbench

In addition to other advantages, water was utilized as a basic fluid in the creation of nanofluids. Its primary benefit is that it is readily accessible, inexpensive, and has strong heat transfer and cooling capabilities. The properties are: density (g/ m^3) = 0.999, specific heat (Cp) (J/kg.K) = 4181, boiling point (℃) = 100, viscosity (kg/m.s) and thermal conductivity (k) (W/m.K) = 0.6.

4.1 Concentration of CuO Nanoparticles

Five distinct concentrations of this kind of nanofluid were also tested on surfaces that had fins of various geometric forms. These were as follows in Tables 3 to 5:

Table 3. The concentrations of Nanofluids (CuO+water) on surfaces where the fins have a triangular form

Triangular Shape of Fins	**Water**	**Water+CuO (0.3)**	**Water+CuO (0.6)**	**Water+CuO (0.1)**	**Water +CuO (0.12)**	**Water +CuO (0.14)**
HTC $\left(\mathrm{kW/m^2 \cdot K}\right)$	0.799705	0.8987684	0.930398	0.907495	0.8033899	0.82969
q" $\left(\mathrm{kW/m^2}\right)$	75.964	85.374	88.3785	86.20301	76.314	78.8125
V(m/s)	0.136846	0.0031605	0.0030983	0.006300	0.0041423	0.002995
P(Pascal)	189.945	194.5142	196.8424	200.5629	202.73505	205.47855
CP(J/kg.K)	4179	4168.083	4157.166	4142.61	4135.332	4128.054
k(W/m · K)	0.61281	0.607307	0.6028301	0.596287	0.5932570	0.5900072
$\rho\left(\mathrm{kg/m^3}\right)$	999	1052.030	1030.018	1013.509	1063.036	1074.042

Table 4. The different concentrations of Nano fluids (CuO+water) on surfaces with square shape of fins

Square Shape of Fins	**Water**	**Water+CuO (0.3)**	**Water+CuO (0.6)**	**Water+CuO (0.1)**	**Water +CuO (0.12)**	**Water +CuO (0.14)**
HTC $\left(\mathrm{kW/m^2 \cdot K}\right)$	0.85385	0.842283	0.8677177	0.827403	0.91234882	0.9095222
q" $\mathrm{kW/m^2}$)	81.1075	80.0085	82.4245	78.595	86.664	86.395508
V(m/s)	0.12475	0.006932	0.00442227	0.005725	0.00488325	0.0045044
P(Pascal)	183.491	189.377	195.61	199.6166	202.16142	203.88174
CP(J/kg.K)	4179	4168.083	4157.166	4142.61	4135.332	4128.0542
k(W/m.K)	0.613	0.607878	0.60307	0.596334	0.59325707	0.5900077
$\rho\left(\mathrm{kg/m^3}\right)$	999	1052.030	1030.018	1013.509	1063.036	1074.042

In the context of nanofluids used for enhancing heat transfer, the concentration of CuO nanoparticles plays a critical role in determining the thermal performance of the fluid. Nanofluids are suspensions of nanoparticles in a base fluid, typically water or oil, and they are known for their improved thermal properties compared to the base fluid alone. One of the primary mechanisms through which nanofluids enhance heat transfer is by increasing the thermal conductivity of the base fluid. The addition of CuO nanoparticles to the fluid increases its effective thermal conductivity. The thermal conductivity enhancement is generally proportional to the concentration of nanoparticles. Higher concentrations of CuO nanoparticles result in a greater enhancement of thermal conductivity, leading to improved heat transfer rates. Nanofluids can enhance convective heat transfer due to their improved thermal properties. The concentration of CuO nanoparticles influences the convective HTC of the nanofluid. Higher

concentrations of nanoparticles can lead to more significant enhancements in convective HTC, especially in forced convection applications. There is typically an optimum concentration of nanoparticles that maximizes heat transfer enhancement. If you add more nanoparticles than this critical concentration, they might not make a big difference in how well heat moves, and they might even cause problems like particles sticking together, which could hurt the fluid's stability and heat transfer properties. While increasing the concentration of CuO nanoparticles enhances thermal conductivity and heat transfer, it can also increase the viscosity of the nanofluid. Higher viscosity can lead to increased pumping power requirements and a pressure drop in the fluid flow system, which may offset the benefits of improved heat transfer. It's important to balance the desired heat transfer enhancement with the practical considerations of fluid viscosity. The concentration of nanoparticles can affect the stability of the nanofluid. Agglomeration or sedimentation of nanoparticles can occur at high concentrations, leading to reduced stability and heat transfer performance.

Table 5. The different concentrations of Nano fluids (CuO+water) on surfaces with circular shape of fins

Circular Shape of Fins	**Water**	**Water+CuO (0.3)**	**Water+CuO (0.6)**	**Water+CuO (0.1)**	**Water +CuO (0.12)**	**Water +CuO (0.14)**
HTC $\left(\mathrm{kW/m^2 \cdot K}\right)$	0.90018	0.7771977	0.81219	1.019229	1.0977893	1.0430889
q" $\left(\mathrm{kW/m^2}\right)$	85.50899	73.826	78.005	96.816	104.279	99.083
V(m/s)	0.002255	0.00232	0.00225	0.002235	0.002114	0.002435
P(Pascal)	191.0448	193.8825	196.6	201.3895	204.0587	205.77826
CP(J/kg.K)	4179	4168.083	4157.166	4142.608	4135.332	4128.0542
k(W/m.K)	0.612717	0.607617	0.6027825	0.596518	0.593257	0.590007
$\rho\left(\mathrm{kg/m^3}\right)$	999	1052.030	1030.018	1013.509	1063.036	1074.042

Figures 6-9 show the fluent program contours for various nanofluid CuO+ water concentrations and their corresponding attributes.

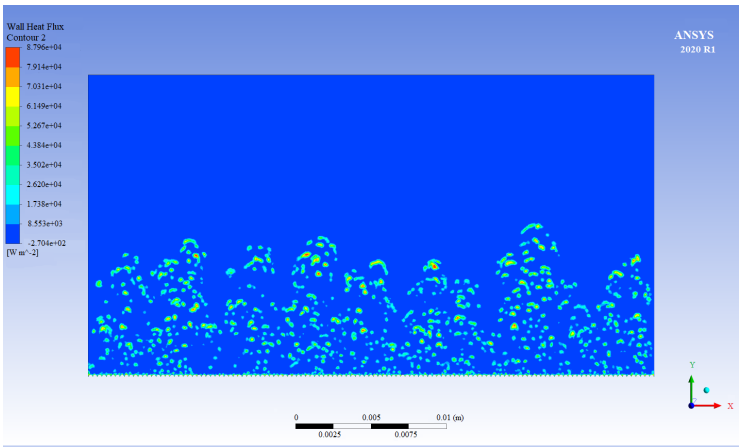

Figure 6. Contours of wall heat flux for CuO+water at 1.2% vol. with square fins

When considering the use of CuO nanoparticles in nanofluids or any other application, it's important to also evaluate their toxicity. While CuO nanoparticles offer several advantages in terms of heat transfer enhancement and other properties, their potential toxicity can raise concerns, especially in terms of human health and environmental impact. CuO nanoparticles can pose health risks if they are inhaled, ingested, or come into contact with the skin in sufficient quantities. Prolonged or high-level exposure to CuO nanoparticles may lead to respiratory problems, skin irritation, and other adverse health effects. CuO nanoparticles can also have environmental implications. The toxicity of CuO nanoparticles can vary depending on factors such as particle size, surface area, and surface chemistry. Smaller nanoparticles generally have higher surface area-to-volume ratios, which can enhance their reactivity and potential toxicity compared to larger particles. The route of exposure to CuO nanoparticles can influence their toxicity. Regulatory agencies in different countries have established guidelines and regulations concerning the use of nanoparticles, including CuO nanoparticles.

Figure 10 illustrates how surfaces with square, circular, and triangular fins correspond to concentration and HTC.

Keep in mind that the surfaces with circular fins and a proportion of CuO+water nanofluid at the optimum concentrations were (1.2 percent volume) (122 percent).

Heat flow and concentration are displayed on surfaces with square, circular, and triangle fins in Figure 11.

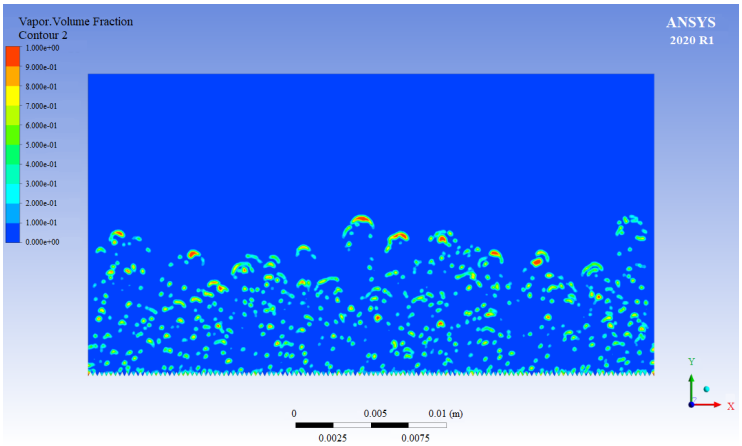

Figure 7. Counter of vapor volume fraction for CuO+water at 0.3% vol. with triangular fins

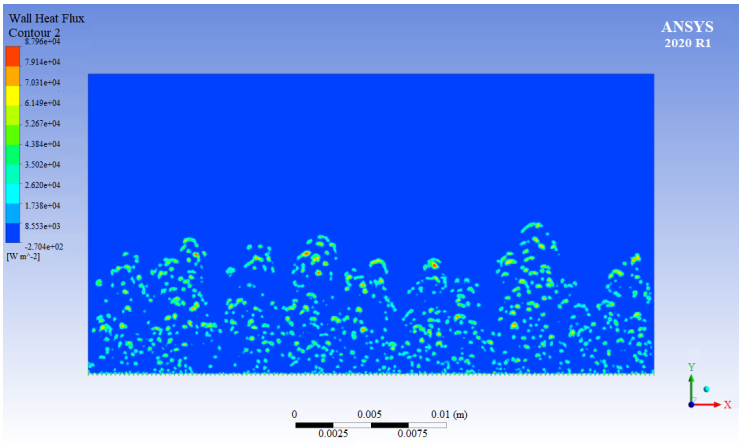

Figure 8. Counter of wall heat flux for CuO+water at 1.2% vol. with circular fins

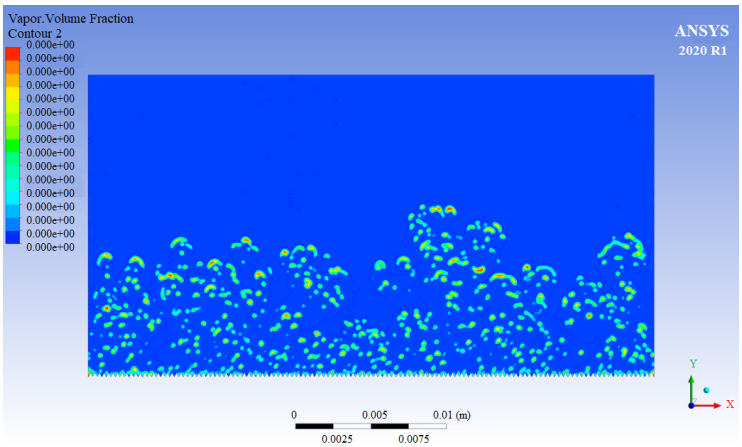

Figure 9. Counter of fraction for vapor volume for CuO+water at 1.2% vol. with triangular fins

It should be noted that the surfaces with circular fins and the greatest concentrations of CuO+water nanofluid were (1.2 percent volume) and (122 percent).

4.2 Fins Shape Effect

In this investigation, three surface types with various fin geometric forms were employed:

4.2.1 Triangular shape

(1) The surfaces featuring triangular fins, measuring 0.3 mm for the triangle's height and base length.

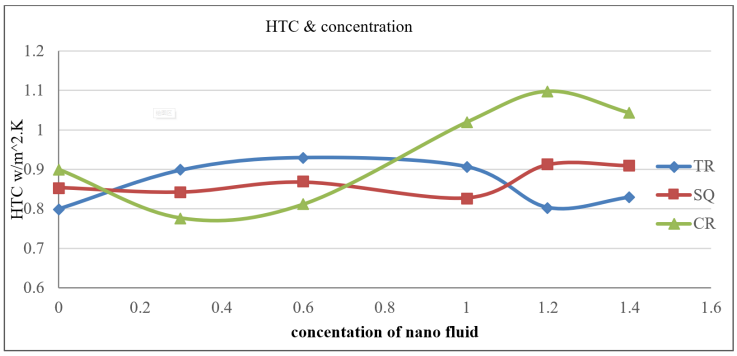

Figure 10. The different concentrations of the (CuO+water) on different fins surfaces

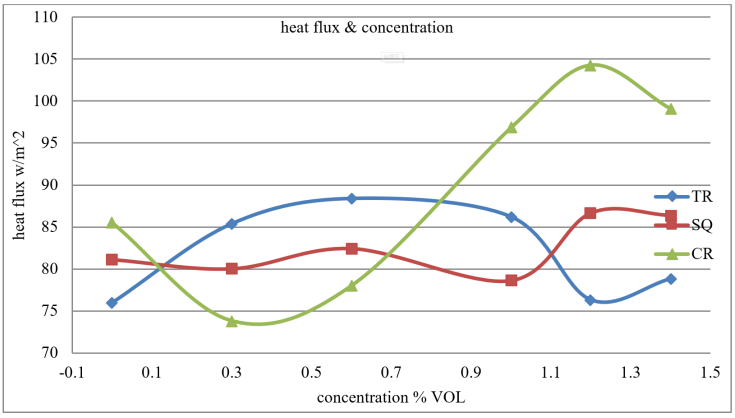

Figure 11. The different concentrations of the (CuO+water) on different fins surfaces

(2) We employed (150774) nodes and (74669) items in this investigation.
In Figure 12, the HTC on the surface with a triangle fin shape is exhibited using CuO+water nanofluid.

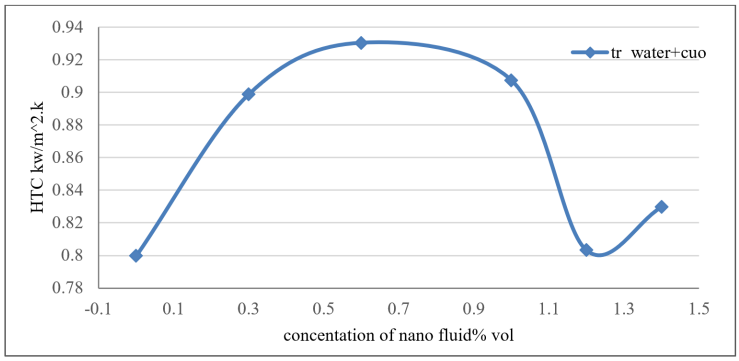

Figure 12. The different concentrations of the (CuO+water) Nanofluid on the surfaces with triangular fins

4.2.2 Square shape

(1) The surface has square fins with diameters of 0.30 mm.
(2) We utilized (150408) nodes and (74442) items in this investigation.
The HTC on the surface with the shape of square fins is depicted with (CuO+water) nanofluid in Figure 13.

4.2.3 Circular shape

(1) The surfaces with round fins have a diameter of 0.30 mm.
(2) In this investigation, we employed (161978) nodes and (159945) elements.
The HTC is depicted with CuO+water nanofluid on the surface with circular fins in Figure 14.

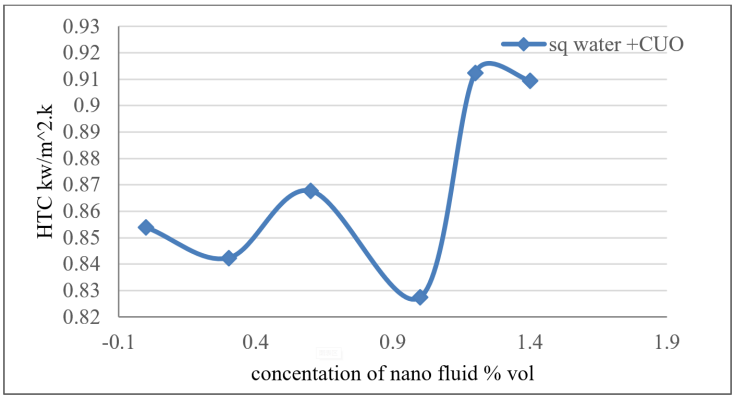

Figure 13. The different concentrations of the (CuO+water) Nanofluid on the surfaces with square geometric shapes of fins

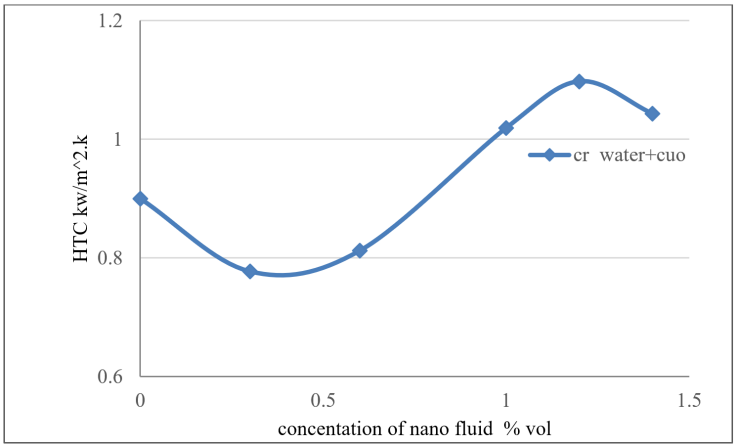

Figure 14. The different concentrations of the (CuO+water) Nanofluid on the surfaces with circular fins

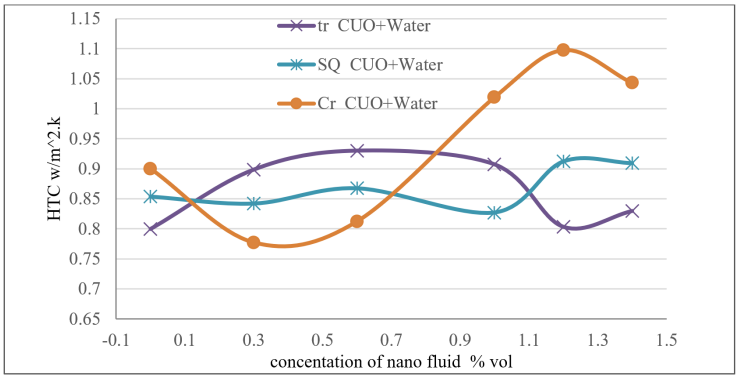

Figure 15. The different concentrations of the (CuO+water) Nanofluid on the different fins

4.3 Comparison

The processors of cooling transfer and heat transfer use water as the foundation fluid. Figure 15 illustrates how HTC uses (CuO+water) nanofluid on a surface with various fin shapes.

The findings obtained from HTC using CuO+water nanofluid at a concentration of 1.2% vole and a percentage of 122% were best achieved by the fins with circular forms.

5 Conclusions and Recommendations

Adding more CuO nanoparticles to nanofluids improves their ability to conduct heat, their convective HTC, and their overall heat transfer rates. However, there is typically an optimal concentration beyond which further addition

of nanoparticles may not yield significant improvements in thermal performance. Balancing the concentration of CuO nanoparticles is crucial to optimizing heat transfer enhancement while considering practical factors such as fluid viscosity, stability, and cost-effectiveness. CuO nanoparticles can pose health risks if exposure occurs through inhalation, ingestion, or dermal contact. Understanding the factors influencing their toxicity, such as particle size, surface area, and exposure routes, is crucial for implementing appropriate safety measures and regulatory compliance. CuO nanoparticles can have adverse effects on the environment if released into soil, water, or ecosystems.

The outcomes demonstrate that, for the basic liquid, water, surfaces featuring circular fins produced the best overall results. The results showed that the optimal concentrations for CuO+water nanofluid for surfaces with square and circular fins were 1.2% volume, whereas 0.6% volume was the best concentration for surfaces with triangular fins. When using ethylene glycol as a base fluid, the effect of using nanofluids ($\mathrm{CuO} + \mathrm{C_2H_6O_2}$) was negative on surfaces with square fins. On surfaces with circular and triangular fins, the best results are obtained when using $\mathrm{CuO} + \mathrm{C_2H_6O_2}$ nanofluid at a concentration of 1% vole for the surface with circular fins and at a concentration of 0.6% vole for triangular fin surfaces.

It is recommended to predict the processes of heat transport and boiling by numerical simulations with other kinds of nanofluids at varying concentrations, such as SIC and $\mathrm{ZrO_2}$. Also, using various types of basic fluids, such as refrigerant R134a, as well as combining these fluids with varying concentrations of nanofluids, and knowing the influence of this on the phenomena associated with boiling. In the future, researchers might look into how to use CuO nanoparticles in nanofluids that have different base fluids (like water, oils, or ethylene glycol) and different substrates (like metals, ceramics, or polymers). This would help broaden the applicability of CuO nanofluids and provide insights into their thermal performance under diverse conditions. Investigating the long-term stability and reliability of CuO nanofluids under various operating conditions is essential for practical applications. To make sure that nanofluid-based heat transfer systems keep working well, researchers could look at how nanoparticles stick together, settle, and break down over long periods of time. Further research is needed to comprehensively assess the environmental and health implications of CuO nanofluids throughout their lifecycle. This includes studying nanoparticle release, transport, and fate in the environment, as well as evaluating potential risks to human health and ecosystems.

Data Availability

The data used to support the findings of this study are available from the corresponding author upon request.

Conflicts of Interest

The authors declare that they have no conflicts of interest.

References

[1] E. I. Eid, R. A. Khalaf-Allah, and M. Tolan, "Enhancement of heat transfer characteristics of nucleate pool boiling by addition of nano-metal particles to the refrigerant 134a," *Int. J. Sci. Eng. Res.*, vol. 9, no. 8, pp. 857–864, 2018.

[2] M. S. Kamel and F. Lezsovits, "Enhancement of pool boiling heat transfer performance using dilute cerium oxide/water nanofluid: An experimental investigation," *Int. Commun. Heat Mass Transf.*, vol. 114, p. 104587, 2020. https://doi.org/10.1016/j.icheatmasstransfer.2020.104587

[3] M. M. Sarafraz and F. Hormozi, "Experimental investigation on the pool boiling heat transfer to aqueous multi-walled carbon nanotube nanofluids on the micro-finned surfaces," *Int. J. Therm. Sci.*, vol. 100, pp. 255–266, 2016. https://doi.org/10.1016/j.ijthermalsci.2015.10.006

[4] S. Z. Xie, M. N. Jiang, H. J. Kong, Q. Tong, and J. Y. Zhao, "An experimental investigation on the pool boiling of multi-orientated hierarchical structured surfaces," *Int. J. Heat Mass Transf.*, vol. 164, p. 120595, 2021. https://doi.org/10.1016/j.ijheatmasstransfer.2020.120595

[5] S. Y. Chun, I. C. Bang, Y. J. Choo, and C. H. Song, "Heat transfer characteristics of Si and SiC nanofluids during a rapid quenching and nanoparticles deposition effects," *Int. J. Heat Mass Transf.*, vol. 54, no. 5-6, pp. 1217–1223, 2011. https://doi.org/10.1016/j.ijheatmasstransfer.2010.10.029

[6] B. Touhami, A. Abdelkader, and T. Mohamed, "Proposal for a correlation raising the impact of the external diameter of a horizontal tube during pool boiling," *Int. J. Therm. Sci.*, vol. 84, pp. 293–299, 2014. https://doi.org/10.1016/j.ijthermalsci.2014.05.023

[7] H. Jafari Zandabad, L. Jahanshaloo, H. Aminfar, and M. Mohammadpourfard, "Experimental study of the effects of quadrupole magnetic field and hydro-thermal parameters on bubble departure diameter and frequency in a vertical annulus," *Exp. Heat Transf.*, vol. 35, no. 3, pp. 341–368, 2021. https://doi.org/10.1080/08916152.2021.1873877

[8] A. N. A. Saieed, M. A. Mashkour, H. M. Hussain, and L. J. Habeeb, "Numerical investigations of multiphase pool boiling in microchannels with several cooling materials," *J. Mech. Eng. Res. Dev.*, vol. 44, no. 3, pp. 219–230, 2021.

[9] H. H. Fadhl, A. Daneh-Dezfuli, and L. J. Habeeb, "Pool boiling heat transfer enhancement using nano-fluids with ethylene-glycol base fluid and micro finned surface," *Int. J. Multidiscip. Sci. Adv. Technol.*, vol. 3, no. 1, pp. 26–39, 2022.

[10] H. S. Majdi, H. M. Abdul Hussein, L. J. Habeeb, and D. Zivkovic, "Pool boiling simulation of two nanofluids at multi concentrations in enclosure with different shapes of fins," *Mater. Today Proc.*, vol. 60, no. 3, pp. 2043–2063, 2022. https://doi.org/10.1016/j.matpr.2022.01.290

[11] H. H. Fadhl and L. J. Habeeb, "Enhancement of pool boiling heat transfer through micro-finned surfaces and Al_2O_3-water nanofluids: A numerical study," *J. Sustain. Energy*, vol. 3, no. 1, pp. 30–45, 2024. https://doi.org/10.56578/jse030103

[12] L. S. Tong and Y. S. Tang, *Boiling Heat Transfer And Two-Phase Flow*. Taylor & Francis, 1997. https://doi.org/10.1201/9781315138510

[13] I. L. Pioro, W. Rohsenow, and S. S. Doerffer, "Nucleate pool-boiling heat transfer. II. assessment of prediction methods," *Int. J. Heat Mass Transf.*, vol. 47, no. 23, pp. 5045–5057, 2004. https://doi.org/10.1016/j.ijheatmass transfer.2004.06.020

[14] D. Wen and Y. L. Ding, "Experimental investigation into the pool boiling heat transfer of aqueous based γ-alumina nanofluids," *J. Nanoparticle Res.*, vol. 7, pp. 265–274, 2005. https://doi.org/10.1007/s11051-005-3 478-9

[15] G. P. Narayan, K. B. Anoop, G. Sateesh, and S. K. Das, "Effect of surface orientation on pool boiling heat transfer of nanoparticle suspensions," *Int. J. Multiphase Flow*, vol. 34, no. 2, pp. 145–160, 2008. https://doi.org/10.1016/j.ijmultiphaseflow.2007.08.004

[16] P. Vassallo, R. Kumar, and S. D'Amico, "Pool boiling heat transfer experiments in silica–water nano-fluids," *Int. J. Heat Mass Transf.*, vol. 47, no. 2, pp. 407–411, 2004. https://doi.org/10.1016/S0017-9310(03)00361-2

[17] I. C. Bang and S. H. Chang, "Boiling heat transfer performance and phenomena of Al_2O_3–water nano-fluids from a plain surface in a pool," *Int. J. Heat Mass Transf.*, vol. 48, no. 12, pp. 2407–2419, 2005. https://doi.org/10.1016/j.ijheatmasstransfer.2004.12.047

[18] W. M. Rohsenow, "A method of correlating heat transfer data for surface boiling of liquids," *Trans. ASME*, vol. 74, pp. 969–976, 1952.

[19] N. Zuber, "Hydrodynamic aspects of boiling heat transfer," *Phys. Math.*, 1959. https://doi.org/10.2172/4175511

[20] "Release 15.0 - contains proprietary and confidential information of ANSYS, Inc. and its subsidiaries and affiliates," 2017. http://storage.ansys.com/doc_assets/ril_docs/RIL_182.pdf

[21] H. Salehi and F. Hormozi, "Prediction of Al_2O_3–water nanofluids pool boiling heat transfer coefficient at low heat fluxes by using response surface methodology," *J. Therm. Anal. Calorim.*, vol. 137, pp. 1069–1082, 2019. https://doi.org/10.1007/s10973-018-07993-w